

Nonlinear Wave Process Revealed in the Spectra of Stimulated Brillouin Scattering

J. Handke, S. A. H. Rizvi,^(a) and B. Kronast

Experimentalphysik V, Ruhr-Universität, D-4630 Bochum, Federal Republic of Germany

(Received 10 May 1983)

Stimulated Brillouin scattering spectra observed from homogeneous and extended target plasma being irradiated with CO₂ laser pulses reveal the presence of ion trapping, the onset of which coincides with a pronounced deviation from the steep stimulated Brillouin scattering increase with laser power. The evaluation of spectra permits the direct measurement of the amplitude of the backscattering ion-acoustic wave and it also provides information on the deformation of the ion velocity distribution under the influence of this wave.

PACS numbers: 52.35.Mw, 52.25.Ps, 52.40.Db, 52.70.Kz

Because of its importance for laser fusion, stimulated Brillouin scattering (SBS) has been investigated extensively. However, even if only so-called model experiments are compared in which CO₂ laser beams are interacting with preformed target plasmas in order to provide defined scattering conditions, the SBS results display a wide scatter as has been shown in the survey article of Chen¹ and the work of Handke² and Handke, Rizvi, and Kronast.³ While in the latter papers^{2,3} an explanation is given for the wide scatter of SBS threshold, it is the purpose of this paper to report on a nonlinear process which reveals itself in SBS spectra. It initiates the deviation from the steep SBS increase with laser intensity which has been viewed as an indication for SBS saturation at low backscattering level in some of the experiments compared in Refs. 1-3.

The experimental setup was the same as has been described in detail already.²⁻⁴ The CO₂ laser beam impinging onto the homogeneous and fully ionized hydrogen plasma of a dynamic *z* pinch at $1.6 \times 10^{19} \text{ cm}^{-3}$ number density was tailored to approach the usual assumptions of theory of a monochromatic and plane wave and produced in excess of $10^{10} \text{ W cm}^{-2}$ power density in a train of nanosecond pulses separated by 16.7 ns. Incident and total backscattered radiation as well as the intensity in the five spectral channels of the array detector were recorded with 100-ps pyrodetectors and displayed on a Tektronix model 7104 oscilloscope. In addition to these time-resolved measurements of SBS spectra, a portion of the spectrometer output was split off and recorded time integrated in each shot by a Pyricon ir camera.

Spectra obtained from the array detector for backscattering levels below 5%⁵ showed a narrow SBS feature which was red shifted by about 17 GHz from the *P*(20) CO₂ laser line. Apart from their somewhat inferior spectral resolution, these spectra showed the same features as those

of the time integrated measurements, examples of which can be found in Refs. 2, 3, and 5. By a ruby-laser light scattering investigation of the SBS volume^{6,7} and by investigation of Doppler shifts and SBS red shift separately⁵ with the help of the interaction model developed in Refs. 2 and 3, Doppler-shift contributions to the spectra could be ruled out for the 80-ns resting phase of the *z*-pinch plasma even under the influence of those CO₂ laser pulses which resulted in backscattering levels well above 10% and the SBS spectra of which displayed features different from those obtained at levels below 5%. The temporal development of the spectrum of such an SBS pulse is depicted in Fig. 1. The curves plotted represent best-fitting curves to the array readouts of a single shot which are shown shaded for one case. The best fit was not only based on the channel spacing of 2.2 GHz but also on two additional conditions: First, the time-integrated spectrum corresponds to the energy spectrum recorded simultaneously by the ir camera with 0.6-GHz resolution showing only two spectral peaks. Secondly, the frequency-integrated time development corresponds to that of the SBS monitor, recording total backscattering. While the frequency separation of sidebands was reproducible, their intensity ratio covered a range from well below to above unity. The temporal development of the SBS spectrum in Fig. 1 shows the development of a lower and upper sideband located symmetrically relative to the ion-acoustic wave frequency ν_{ia} which was evaluated on the base of electron and ion temperatures. Figure 2 representing a section at 0.6 ns visualizes these features. This spectral splitting can be seen as a consequence of ion trapping in the potential distribution of the backscattering ion-acoustic wave such as has been observed and dealt with extensively in connection with microwave experiments.⁸ The mere occurrence of two sidebands can be understood

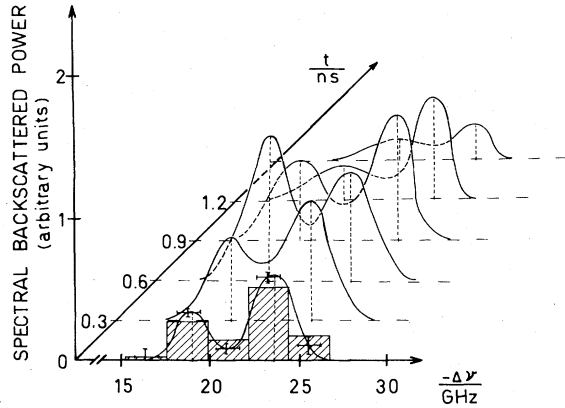


FIG. 1. The temporal development of an SBS spectrum measured with a pyroelectric array detector of less than 100-ps response time. The red-shifted spectral power is plotted vs the frequency difference to the incident CO₂ P(20) laser line. The curves represent best fits to the array read outs, an example of which is shown shaded. The best fits are obtained for the additional conditions that the frequency-integrated signals correspond to the time dependence of the SBS monitor signal and that the time-integrated spectra agree with the energy spectrum recorded simultaneously by an ir camera system. The error bars given in the curve at $t=0$ are relative standard deviations and are representative also for the other curves.

in a simple picture. The trapped ions are oscillating at the bottom of the sinusoidal potential distribution such as in a harmonic oscillator and their bounce frequency is immediately derived from this principle to be

$$\nu_B = (k_{ia}/2\pi)(e\varphi_0/m_i)^{1/2} \quad (1)$$

(φ_0 is the wave potential, k_{ia} and ω_{ia} wave number and frequency of the ion wave, m_i ion mass and e the elementary charge). The ions bouncing back and forth in the potential troughs are exchanging energy with the wave at the cadence of the bounce frequency ν_B and are, thus, modulating the carrier wave with ν_B . The Fourier transform of this time dependence leads to sidebands in the frequency spectrum which are separated by $2\nu_B$. Thus, from the frequency difference of the two sidebands the bounce frequency ν_B can be measured. As long as the density modulation δn_{ia} caused by the ion-acoustic wave is small compared to the plasma density n_e the relation

$$\delta n_{ia}/n_e = e\varphi_0/\kappa T_e \quad (2)$$

holds, where κT_e is the thermal electron energy. Combining both equations and setting $\nu_e^2 = \kappa T_e /$

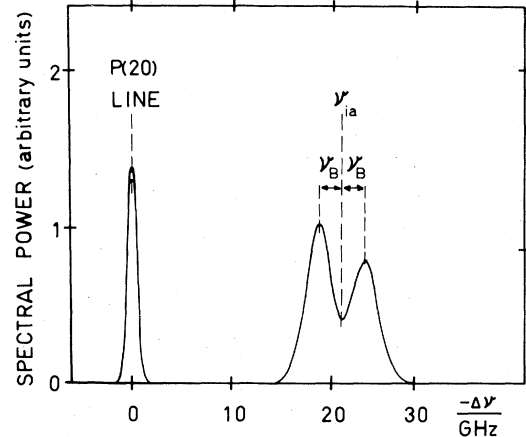


FIG. 2. A section of the SBS spectral evolution of Fig. 1 at time 0.6 ns. Upper and lower sideband are separated from the ion-acoustic wave frequency ν_{ia} by the bounce frequency ν_B . Added is also the narrow P(20) line of the incident laser.

m_e gives

$$\nu_B = \frac{k_{ia}}{2\pi} v_e \left(\frac{m_e}{m_i} \right)^{1/2} \left(\frac{\delta n_{ia}}{n_e} \right)^{1/2} \quad (3)$$

This equation permits the determination of an important parameter such as the density amplitude of the backscattering ion-acoustic wave from a relatively precise frequency measurement. This was done and the dependence of $\delta n_{ia}/n_e$ on the backscattering level R is plotted in Fig. 3. The density modulation is only on the order of a few percent; however, completely unexpected is the decrease in amplitude of the backscattering wave while the backscattered power P_{SBS} itself increases. The explanation for this contradictory behavior is provided by the observation that the length of the backscattering ion wave is increasing with P_{SBS} and is overcompensating the de-

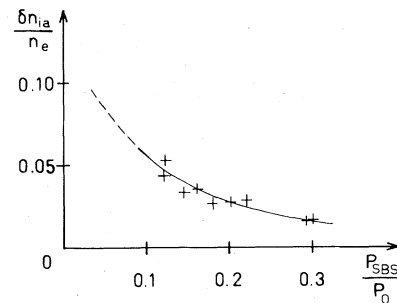


FIG. 3. The density amplitude of the backscattering ion-acoustic wave δn_{ia} normalized to the mean electron density n_e of the target plasma plotted vs the relative SBS power.

crease in $\delta n_{ia}/n_e$. This has been documented by Gellert and Kronast.^{6,9} In addition to this dependence on backscatter level, a confirmation of also the absolute value of the above $\delta n_{ia}/n_e$ in the overlapping region of $0.12 \leq P_{SBS}/P_0 \leq 0.15$ can be derived in the following manner: The values of Fig. 3 represent spatial and temporal peak values since they are derived from a nonlinear wave process. The values reported in Refs. 6 and 9 as a function of backscatter level are spatial and temporal mean values. By use of the most reliable data of Refs. 6 and 9, which were obtained from an evaluation of SBS backscatter with an analytical expression for the scattering off a coherent wave, these mean values differ in a first coarse approach by a factor of 2 from their peak values. These coarse peak values confirm the $\delta n_{ia}/n_e$ values of Fig. 3 within their error bars of about $\pm 40\%$. Obtained by a completely different measurement technique, this agreement both in magnitude and in its dependence on backscattering level represents an independent support for the validity of the explanation.

For the purpose of explaining and for a coarse estimation of the mere splitting of the SBS spectrum, the simple model above may suffice. However, in order to evaluate details of these spectra a sophisticated theoretical description is required. Such a theory is available in the work of Mima and Nishikawa.¹⁰ Though their treatment deals with a high-amplitude electron-plasma wave it can—in the author's words—nonetheless “be applied to the case in which a large-amplitude ion wave is present in a two-temperature plasma ($T_e \gg T_i$).” If $T_e/T_i \geq 4$ can be considered sufficient to meet the above condition, conclusions can now be drawn also from the observed asymmetry of the spectral sidebands, different cases of which are represented by the various time sections of Fig. 1. According to the above theory the intensity ratio of lower to higher sideband gives information on the deviation of the ion velocity distribution function from a Maxwellian in the vicinity of the wave velocity. If it is less than unity the number density of ions exceeds that of a Maxwellian and vice versa. In this way, the spectrum at 0.0 ns in Fig. 1 represents a case in which ion trapping must have filled up the ion number density above the equilibrium value, while at 0.6 ns a particle deficiency must have developed, subsequently again followed by a reversal. In the above sense, a modulation of the ion number density must be inferred from the measured spectral evolution.

The above theory also explains the somewhat puzzling situation that the bounce motion obviously is not suppressed, although the ion collision frequency ν_i somewhat exceeds the bounce frequency ω_B . However, collisions will affect the process only¹⁰ if $\nu_i/\omega_B > (v_t/v_i)^2$, where v_t is the trapping velocity and v_i the thermal ion velocity. For the conditions investigated v_t exceeds v_i by so much that the above limit was not reached.

The position of the sharp bend in the backscattering curves referred to in Refs. 2–4 can also be explained by ion trapping: Before the bouncing period, SBS rises with exponentiation times on the order of 10 ps causing an overshoot to δn_{ia} values which make possible ion trapping from the highly populated thermal region of the ion distribution. The $\delta n_{ia}/n_e$ values required can be estimated from a relation given by Dawson, Krueer, and Rosen¹¹ as

$$\frac{\delta n_{ia}}{n_e} = \frac{1}{2} \left[\left(1 + \frac{3T_i}{T_e} \right)^{1/2} - \left(\frac{3T_i}{T_e} \right)^{1/2} \right]^2. \quad (4)$$

The associated ion acceleration represents considerable energy loss to the wave and its density amplitude is lowered to values well below the trapping limit [Eq. (4)]. This onset of additional damping causes the observed bend in backscattering curves. With use of T_e/T_i values determined in Refs. 2, 3, and 6 for the conditions of the bend, the overshoot density amplitude required for trapping can be estimated by Eq. (4) to be $\delta n_{ia}/n_e \approx 8 \times 10^{-2}$. In fact, an extrapolation of the results in Fig. 3 to backscatter levels below 0.1 leads to such values if it is kept in mind that the initial density amplitude at the onset of trapping is higher than that during the subsequent phase of bouncing. The wave damping during bouncing is not caused by ion trapping but has been shown in Refs. 6 and 9 to be due to harmonic production of the ion wave. In this sense, initial ion trapping merely initiates the nonlinear damping mechanism which causes the SBS increase with laser intensity to approach the Manley-Rowe limit at a greatly reduced slope.²⁻⁴ Direct experimental evidence for harmonic production has been reported by Walsh and Baldis¹² for a different kind of target plasma. Though not considered by these authors, Fig. 2(c) of their paper indicates that the above motion of trapped ions becomes evident in the modulation of the streak at $k/k_{\text{pump}} = 2$.

In summarizing, our view of the processes suggested by the observations is the following: The rapid SBS rise preceding the bouncing period

causes an initial overshoot to δn_{ia} values making possible ion trapping. Only the associated initial ion acceleration causes strong losses to the ion wave energy, lowering $\delta n_{ia}/n_e$ well below values necessary for strong ion trapping. At these low values, on the order of a few percent, bouncing occurs and during this phase the dominant loss mechanism is provided by harmonic damping of the ion wave. The initial phase of ion trapping must be short compared to the subsequent bouncing period because the values of $\delta n_{ia}/n_e$ observed for the phase of maximum SBS are well below those required for trapping.⁹

We should like to thank our colleague Dr. B. Gellert for cooperation and Dr. D. Rusbült for providing valuable advice and hardware. Our appreciation for valuable discussions on theoretical matters with Professor H. Schamel and Dr. P. Shukla must also be expressed here. Our research work was performed under the auspices of the Sonderforschungsbereich Nr. 162 Plasmaphysik Bochum/Jülich. The contribution of one of us (S.A.H.R.) was made possible by a scholarship of the German Exchange Service (Deutsche Akademische Austauschdienst).

^(a)On leave of absence from the Pakistan Atomic Energy Commission, Pinstech, Nilore, Rawalpindi,

Pakistan.

¹F. F. Chen, in *Proceedings of the International Conference on Plasma Physics, Nagoya, Japan, April 7-11, 1980*, edited by K. Takayama (Fusion Research Association Japan, Nagoya, 1980), p. 345.

²J. Handke, Sonderforschungsbereich Plasmaphysik Bochum/Jülich, Ruhr-Universität Bochum Report No. 82-N3-108, 1982 (unpublished).

³J. Handke, S. A. H. Rizvi, and B. Kronast, *Laser Part. Beams* 1, 259 (1983).

⁴J. Handke, S. A. H. Rizvi, and B. Kronast, *Appl. Phys.* 25, 109 (1981).

⁵S. A. H. Rizvi, Ph.D. thesis, Ruhr-Universität Bochum, 1983 (unpublished).

⁶B. Gellert and B. Kronast, *Appl. Phys.* (to be published).

⁷B. Gellert, Sonderforschungsbereich Plasmaphysik Bochum/Jülich, Ruhr-Universität Bochum, Report No. 82-N3-109 (unpublished).

⁸T. M. O'Neil, *Phys. Fluids* 8, 2255 (1965); C. B. Wharton, J. H. Malmberg, and T. M. O'Neil, *Phys. Fluids* 11, 1761 (1968); J. Denavit and W. L. Kruer, *Phys. Fluids* 14, 1782 (1971); J. Canosa and J. Gazdag, *Phys. Fluids* 17, 2030 (1974); H. Ikezi *et al.*, *Phys. Fluids* 21, 239 (1978), and many references therein.

⁹B. Gellert and B. Kronast, to be published.

¹⁰K. Mima and K. Nishikawa, *J. Phys. Soc. Jpn.* 30, 1722 (1971), and 33, 1669 (1972).

¹¹J. M. Dawson, W. L. Kruer, and B. Rosen, in *Dynamics of Ionized Gases*, edited by M. Lighthill, I. Imai, and H. Sato (University of Tokyo Press, Tokyo, 1973), p. 47.

¹²C. J. Walsh and H. A. Baldis, *Phys. Rev. Lett.* 48, 1483 (1982).